Control of Type 1 Diabetes Mellitus using Particle Swarm Optimization driven Receding Horizon Controller*

Máté Siket [*,**,†] **Kamilla Novák** [*] **Hemza Redjimi** [†]
József Tar [***] **Levente Kovács** [*,****] **György Eigner** [*,****]

[*] *Physiological Controls Research Center, Óbuda University, H-1034, Budapest, Bécsi street 96/B.*
[**] *ELKH SZTAKI,H-1518 Budapest, P.O. Box 63, Hungary*
[***] *Bejczy Antal Center for Intelligent Robotics, Óbuda University, H-1034, Budapest, Bécsi street 96/B.*
[****] *Biomatics and Applied Artificial Intelligence Institute, Óbuda University, H-1034, Budapest, Bécsi street 96/B.*
[†] *Applied Informatics and Applied Mathematics Doctoral School, Óbuda University, H-1034, Budapest, Bécsi street 96/B.*

Abstract: Receding Horizon Control (RHC), also known as Model Predictive Control (MPC) is one of the most intensively researched areas of control algorithms applied in the artificial pancreas concept. Nevertheless, MPC algorithms have not yet been implemented in commercially available insulin pumps, mainly due to their high computational demand, their less robust nature, and their instability on account of model's uncertainty. In this paper, we present a robust adjustable RHC. The proposed RHC controller was tested under known food inputs by applying a high degree of parameter uncertainty to the virtual patient implemented in the controller to test the robustness of the architecture. A particle swarm optimization method was applied to tune the controller. The so-called identifiable virtual patient (IVP) model was used in the tests, supplemented with food absorption and continuous glucose monitoring sensor model. The implementation was performed in Julia. The results showed that the proposed RHC is sufficiently robust under high food intake and parameter uncertainty.

Keywords: Model predictive control of hybrid systems, Optimal control of hybrid systems, Control in system biology, Nonlinear predictive control, Control of physiological and clinical variables, Type 1 Diabetes Mellitus, Receding horizon control

1. INTRODUCTION

The most promising direction in the management of type 1 diabetes mellitus (T1DM) is the artificial pancreas (AP) concept, where an insulin delivery unit (insulin pump - IP) automatically doses the insulin based on the measured glucose values (provided by eg. continuous glucose monitoring sensor - CGMS) based on advanced control algorithms (Shah et al. (2014)).

The cost function based model based predictive control is a widely applied technique in diabetes management (Doyle et al. (2014)). Many interesting solutions for automated insulin delivery involve a sort of RHC architecture in the blood glucose (BG) management. The main benefit of the method is that multiple goals can be defined as "targets" into the optimization process. The most important metrics are the avoidance of hypoglycemia (BG lower than 70 mg/dL) and increasing the Time-in-Range (TIR). TIR determines how much time a patient spends in the euglycemic range (between 70 mg/dL and 180 mg/dL) during the time when the controller was online or in general sense, while the CGM was worn (Wright et al. (2020)). Many promising MPC algorithms have been recently reported where hypoglycemia has been minimized but also with good TIR (BG spends more than 85% in euglycemic range). Integral MPC (IMPC) is able to operate with acceptable TIR in the presence of disturbances (e.g. from unannounced meal) and model uncertainties (Incremona et al. (2018)). Impulsive zone MPC (IZMPC) aims to provide similar control action like the natural insulin regulation in the β-cells of the pancreas (González et al. (2020)). Other interesting studies showed capabilities which could be embedded into an MPC kind controller (Colmegna et al. (2021)).

⋆ M. Siket, Gy. Eigner, and L. Kovács were supported by the Eötvös Loránd Research Network Secretariat under grant agreement no. ELKH KÖ-40/2020 ('Development of cyber-medical systems based on AI and hybrid cloud methods'). This project has received funding from the European Research Council (ERC) under the European Union's Horizon 2020 research and innovation programme (grant agreement No 679681). Project no. 2019-1.3.1-KK-2019-00007. has been implemented with the support provided from the National Research, Development and Innovation Fund of Hungary, financed under the 2019-1.3.1-KK funding scheme. M. Siket was supported by the ÚNKP-20-3 New National Excellence Program of the Ministry for Innovation and Technology.

It has to be noted that despite the many good applications, MPC based controllers are still not present in the daily practice in insulin pumps as the main control algorithm. Albeit, the new products do have well established predictive features e.g. to estimate the glucose and insulin levels in blood (Breton and Kovatchev (2021)). Clinical studies reported good performance of Omnipod MPC algorithm from both TIR and hypoglycemia points of view (Forlenza et al. (2019)). Two still ongoing clinical study investigate the safety and other aspects of Omnipod MPC – the recent reports introduced good intermediate results (Castle (2021)). Despite the fact that MPC based controllers have not been used in insulin pumps yet, the research directions show that they will and in the near future.

Our group successfully developed robust control algorithms for T1DM by using different techniques e.g. Kovacs et al. (2019) in which a popular tensor product based approach has been used (Hedrea et al. (2021)). In this study, we focused on developing a receding horizon controller (RHC) which can overachieve the performance and stability of classical MPC algorithms (Kwon and Han (2006)). The heuristic "RHC" is an optimal control strategy invented in the late seventies of the last century (Richalet et al. (1978)). It approximates the constant time variable over a distinct grid. In order to provide smooth Euler integration of the state variable of the controlled system over a finite "future horizon" the grid should have a proper resolution. RHC carries out the "optimisation" over this horizon in such a way that it compiles a "cost function" into a sum of non-negative differentiable contributions connected to the individual restrictions, and minimises it, meanwhile it is important to accurately factor in the controlled system's dynamic model as a "constraint". Modelling imprecisions and not observable external disturbances, which can occur in RHC, are offset by making only one step forward along the fully calculated horizon by using the calculated control signal, and initiating the new horizon from the observed actual state.

2. MATERIALS AND METHODS

2.1 Receding Horizon Controller

The formula that mathematically describes the RHC controller can be written as follows:

$$\min_{\substack{\{\mathbf{x}_1,\ldots,\mathbf{x}_{HL}\}\\ \{\mathbf{u}_0\ldots,\mathbf{u}_{HL-1}\}}} \sum_{i=0}^{HL-1} J(\mathbf{x}_i,\mathbf{u}_i) \quad \text{subject to } \frac{\mathbf{x}_{i+1}-\mathbf{x}_i}{\Delta t} - f(\mathbf{x}_i,\mathbf{u}_i) = \mathbf{0}, \tag{1}$$

where $\{t_0, t_1 = t_0 + \Delta t, \ldots, t_{n+1} = t_n + \Delta t, \ldots, t_{HL}\}$ corresponds to the time grid over the finite future horizon, $HL \in \mathbb{N}$, t_0 and t_{HL} are the beginning and the ending time instants of the horizon, accordingly. Equation for motion of the system to be controlled is $\dot{\mathbf{x}}(t) = f(\mathbf{x}(t), \mathbf{u}(t))$, in which $\mathbf{x}(t) \in \mathbb{R}^M$ is the state variable, $\mathbf{u}(t) \in \mathbb{R}^K$ is the control input, and $\mathbf{x}_0 \equiv \mathbf{x}(t_0)$ is the original condition for the system's status. If $\mathbf{x}^N(t_i)$ is the nominal trajectory to be traced, and $\mathbf{x}(t_i)$ defines the executed trajectory, a cost function $J(\mathbf{x}(t), \mathbf{u}(t))$ can be predetermined in each moment of the grid. In (1) the numerical estimation $\frac{\mathbf{x}_{i+1}-\mathbf{x}_i}{\Delta t} \approx f(\mathbf{x}_i, \mathbf{u}_i)$ is applied.

The nominal trajectory is defined to be a constant 90 $[mg/dL]$ BG concentration. An asymmetric quadratic cost function is applied, due to short term deviations from the nominal value poses various threats to the patient. The asymmetry is taken into account with different δ parameters for the hypoglycemic and hyperglycemic ranges as follows:

$$J(y_i, \mathbf{u}_i) = \left(\frac{y^N - y_i}{\delta}\right)^2 \begin{cases} \delta = \delta_{hyper}, & \text{if } y_i \geq y^N \\ \delta = \delta_{hypo}, & \text{otherwise} \end{cases} \tag{2}$$

In order to find the minimum of J, a *"Gradient Descent Algorithm"* is used: an original point is set to $\mathbf{u}(1) = 1$; Let $\mathbf{u}(2) = \mathbf{u}(1) - \alpha \nabla J|_{\mathbf{u}(1)}$ in which $0 < \alpha$. At the point where $\|\nabla J\| = 0$, the algorithm stops. This point matches a local minimum. In respect that the grid points $i, i+1$ of the discretized time approach, over which the estimation of *"forward differences"* for the first order dynamic system of the estimated model is solved $\dot{q} = f(q, u)$ (u defines the control signal). If the state $q[i]$ and the force $u[i]$ values in grid point i are given, the estimation $q[i+1] \approx q[i] + f(q[i], u[i])\Delta t$ can be applied for the next grid point. Therefore, with the presumed force components $\{u[1], \ldots, u[HL-1]\}$ can be filled in over the horizon. If the *"nominal trajectory to be traced"* is known beforehand, the tracking fault components that are produced as the results of these force components $\{q^N[2] - q[2], \ldots, q^N[HL] - q[HL]\}$ can be directly computed and their contribution to the cost function can be added. In the next step the cost calculated over the whole horizon can be minimized by the simple gradient descent method applied for the independent variables $\{u[1], \ldots, u[HL-1]\}$.

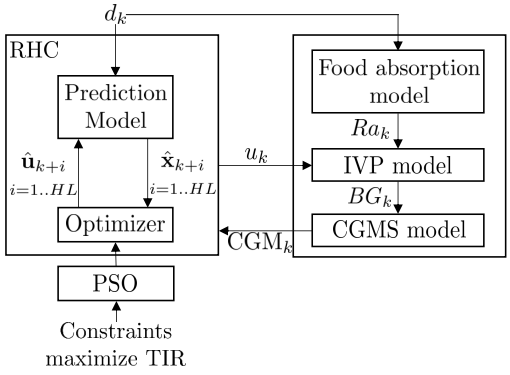

Fig. 1. Diagram of the RHC, PSO and virtual patient.

2.2 Tuning of the RHC

The RHC was tuned with the Particle Swarm Optimization (PSO) method introduced in Kennedy and Eberhart (1995) and Shi and Eberhart (1998). The concept of the algorithm is to create a swarm of particles which move around in the multidimensional problem space whilst competing and sharing information with each other. Each particle has a position and a velocity, which can be calculated as follows:

$$p_{j,d} = p_{j,d} + v_{j,d}, \tag{3}$$

$$v_{j,d} = \omega v_{j,d} + c_1 r_1 (pb_{j,d} - p_{j,d}) + c_2 r_2 (gb_d - x_{j,d}), \tag{4}$$

where the position, velocity and personal best known position of the jth particle in dimension d are denoted

by $p_{j,d}$, $v_{j,d}$ and $pb_{j,d}$. The gb_d is the global best known position among all the particles in dimension d. The ω is the inertia weight which balances the global search and local search, c_1, c_2 are positive acceleration constants, r_1, r_2 are random values in the range [0;1]. The fitness function Ψ, used to evaluate the particles' position, is a function of the TIR of all patients, which penalizes the time spent in hypoglycemia more than the time in hyperglycemia:

$$\Psi = TIR_{hyper} + wTIR_{hypo}, \tag{5}$$

where TIR_{hypo} is the time spent below 70 $[mg/dl]$, TIR_{hyper} is the time spent above 180 $[mg/dl]$ and w is a constant bigger than 1. We found that $w = 5$ is where the occurrence of hypoglycemic events is best minimised.

The optimized values are further investigated around their local minimum found by the PSO. Parameter sensitivities are calculated in order to quantify the dependency of the tuned controller parameters on the TIR based total cost. The parameter sensitivities are defined by:

$$s_p = \frac{\Delta\Psi}{\Delta p} \tag{6}$$

$$S_{p_l} = \frac{p_l}{\Psi_l} s_{p_l}, \tag{7}$$

$$S_p^{msqr} = \sqrt{\frac{1}{n_s}\sum_{l=1}^{n_s}(S_{p_l})^2}, \tag{8}$$

where $\Delta\Psi = \Psi_{nom.} - \Psi_l$ is the cost difference observed by making parameter p different from its nominal value $p_{nom.}$, $\Delta p = p_{nom.} - p_l$. The relative or normalized parameter sensitivity is denoted by S_{p_l}, p_l is the l-th sample from the total of n_s samples. The sensitivity of a given p parameter can be quantified in different ways (Brun et al. (2001)), for our purposes we applied the root-mean-square metric (8).

2.3 Diabetes Patient Model

As a good compromise between complexity and accuracy, the so-called IVP model is utilized, extended with the second order carbohydrate absorption submodel of Hovorka et al. (2004).

$$\begin{aligned}\dot{G}(t) &= -(GEZI + I_{EFF}(t)) \cdot G(t) + EGP \\ &\quad + \frac{1}{\tau_D V_G} D_2(t),\end{aligned} \tag{9}$$

$$\dot{I}_{EFF}(t) = -p_2 \cdot I_{EFF}(t) + p_2 \cdot S_I \cdot I_P(t), \tag{10}$$

$$\dot{I}_P(t) = -\frac{1}{\tau_2} \cdot I_P(t) + \frac{1}{\tau_2} \cdot I_{SC}(t), \tag{11}$$

$$\dot{I}_{SC}(t) = -\frac{1}{\tau_1} \cdot I_{SC}(t) + \frac{1}{\tau_1 C_I} \cdot u(t), \tag{12}$$

$$\dot{D}_1(t) = -\frac{1}{\tau_D} D_1(t) + \frac{1000 A_g C}{M_{wG}} d(t), \tag{13}$$

$$\dot{D}_2(t) = -\frac{1}{\tau_D} D_2(t) + \frac{1}{\tau_D} D_1(t), \tag{14}$$

where $G(t)$ is the blood glucose concentration $[mg/dL]$, $I_{EFF}(t)$ is insulin effect $[min^{-1}]$, $I_{SC}(t)$ and $I_P(t)$ represent the subcutaneous and plasma insulin concentrations $[\mu U/mL]$, respectively. The infused insulin $u(t)$ $[\mu U/min]$ serves as the input. The disturbance $d(t)$ $[g]$ (carbohydrate content of the meal) is considered unknown. Parameters related to the insulin effect: τ_1 and τ_2 $[min]$ insulin absorption time constants, p_2 is the kinetic rate for insulin action $[min^{-1}]$, C_I is the insulin clearance $[mL/min]$, S_I is the insulin sensitivity $[mL/\mu U/min]$. The endogenous glucose production is denoted by EGP and $GEZI$ is the glucose effectiveness at zero insulin level. The meal absorption is affected by the τ_D time constant $[min]$, the V_G $[L]$ glucose distribution volume and the A_g $[-]$ carbohydrate utilization constant. Lastly, C and M_{wG} are conversion constants.

2.4 Continuous Glucose Monitoring Model

In order to simulate the characteristics of a modern CGMS, the error model proposed in Vettoretti et al. (2019) is used. The common method is to use an additional compartment, representing the interstitial glucose concentration, which introduces delay (Huyett et al. (2018)). Besides the additional compartment, the model of Vettoretti et al. (2019) uses an uncertainty of calibration and an additive noise term. The additive noise term v is assumed to be an autoregressive process of order two, driven by zero-mean white noise $w \sim \mathcal{N}(0, \sigma^2)$:

$$\dot{IG}(t) = -\frac{1}{\tau_{IG}} IG(t) + \frac{1}{\tau_{IG}} G(t), \tag{15}$$

$$IG_s(t) = (a_0 + a_1 t + a_2 t^2) IG(t) + b_0, \tag{16}$$

$$v(t) = \alpha_1 v(t - T_s) + \alpha_2 v(t - 2T_s) + w(t), \tag{17}$$

$$CGM(t) = IG_s(t) + v(t), \tag{18}$$

where IG is the interstitial glucose concentration, τ_{IG} is the time constant between the blood and the interstitial compartments. IG_s is the interstitial glucose concentration of the sensor. The uncertainty of the sensor calibration is taken into account with parameters: a_0, a_1, a_2 and b_0. The autoregressive process is defined by parameters: α_1 and α_2.

3. RESULTS

The RHC is implemented in Julia language, in *Julia Version 1.6.0*. Google Colaboratory was used for the simulations.

In the controller we utilized an approximate parameter set created by taking the arithmetic mean of the identified parameters of Kanderian et al. (2009). The nominal parameters are summarized in Table 1.

EGP	$GEZI$	V_G	C_I
0.95	$2.52 \cdot 10^{-3}$	21.4	1266.6
τ_1	τ_2	p_2	S_I
70.5	44.4	$1.13 \cdot 10^{-2}$	$4.41 \cdot 10^{-4}$

Table 1. Approximate parameter values used in the controller.

The BG trajectories of the virtual patient cohort are generated by taking samples from a normal distribution $p \sim (\mu_p, \sigma_p^2)$, where μ_p is the arithmetic mean of parameter p, $\sigma_p := 0.25\mu_p$. In other words, a 25% parameter

variability is applied in the virtual patient cohort for all the parameters. The total simulated horizon was 10 hours long in which the parameters do not change significantly according to the literature (Kanderian et al. (2009)). Thus, we decided to use permanent parameter set in this study. In our future work with longer horizon we will consider introducing intraday parameter variation as well. In the 10-hour-long simulated horizon three meals were administered in the $[60, 240, 480]$ $[min]$ time instances with carbohydrate content of $[20, 60, 10]$ $[g]$. These simulated BG trajectories were perturbed by the CGMS model (15)-(18) using the following parameters, based on Vettoretti et al. (2019): $a_0 = 0.95$, $a_1 = 0$, $a_2 = 0$, $b_0 = 7.3$, $\alpha_1 = 1.3$, $\alpha_2 = -0.46$, $\sigma = 3.2$, $T_s = 5$ and $\tau_{IG} = 3.1$.

The optimized values of the controller parameters are shown in Figs. 2-5. Note that on these plots cost represents the total cost associated with a given parameter set of the controller, simulating the full cohort. The total cost is defined by (5). In Fig. 2 an optimal horizon length is found at 32 discrete steps, resulting in a horizon length of 160 minutes, which correlates well with the effect of a typical meal. Shorter horizon lengths can cause postponed hypoglycemia by not taking into account the full effect of higher insulin administration periods during meal intakes. Since the applied RHC does not use an offset-free strategy (Tamayo et al. (2019)) the parameter uncertainty in case of longer horizons can lead to extended hyperglycemic events. With the given implementation we experienced increasing computational cost with longer horizons. Thus, we selected the best length from the selected control quality properties (hypoglycemia, TIR) point of view (Fig. 2.

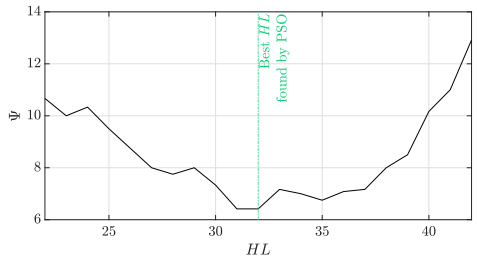

Fig. 2. Fitness function Ψ with respect to HL around its optimum found by PSO.

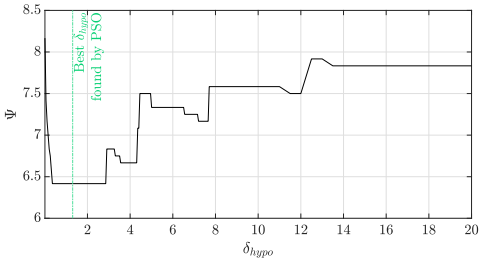

Fig. 3. Fitness function Ψ with respect to δ_{hypo} around its optimum found by PSO.

The δ_{hypo} parameter (Fig. 3) defines a low penalization range for deviations from the nominal value in the negative direction. Since hypoglycemic events are heavily penalized, and the nominal value is relatively close to the lower bound of the TIR, the optimized range is narrow. In Fig. 3 the cost function is flat around the found optimum and non-convex. In Fig. 7 it can be seen that in the simulated horizon hyperglycemic events are sparse, making the controller less sensitive to δ_{hypo} and the cost function non-convex. The applied cost function (5) is non-differentiable, the non-convexity can be further enhanced in the short hyperglycemic section by the CGMS noise. The results of the PSO optimization of the δ_{hyper} parameter can be seen in Fig. 4.

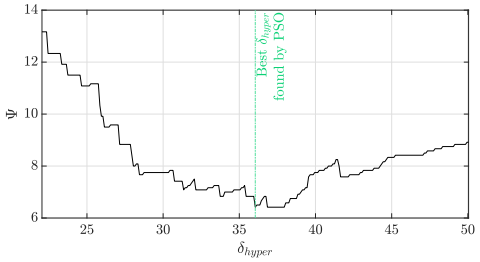

Fig. 4. Fitness function Ψ with respect to δ_{hyper} around its optimum found by PSO.

The α parameter defines the general convergence properties of the gradient descent algorithm. As an upper limit is defined in the RHC for the number of iterations in each time step, low α parameters degrade the convergence. High α values can lead to oscillations around a local optimum and degrade the convergence as well. A lower total cost is found with higher values, as a quick convergence occurs to a neighbourhood of local minimum.

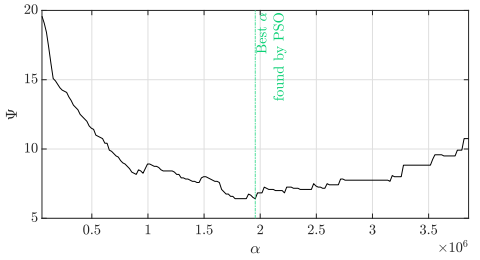

Fig. 5. Fitness function Ψ with respect to α around its optimum found by PSO.

$S_{\delta_{hyper}}$	S_{HL}	S_{α}	$S_{\delta_{hypo}}$
2.0562	1.4774	0.7925	0.1273

Table 2. Calculated parameter sensitivities around their optimized values.

In Table 2 the parameter sensitivities are shown around their optimized values. The largest effect on the TIR metric has the δ_{hyper} and HL parameters. This can be explained by the fact that in the investigated horizon mainly hyperglycemic events occur. The α parameter is found to be the third sensitive in the ranking process, which indicates that relatively large range of α values does not compromise the convergence of the optimizer in a great extent. The least sensitive is found to be the δ_{hypo} parameter, since hypoglycemic events are short. In our further work, further analysis with more patient parameter variability will be carried out, and the outliers of the cohort will be investigated.

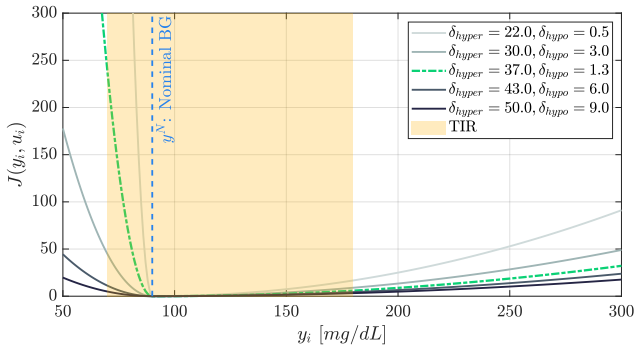

Fig. 6. Applied cost with respect to the measured BG concentration, using different combinations of the δ parameters.

In Fig. 6 the cost function J (2) is shown with respect to the measured BG concentration. The green dashed line represents the optimized cost function calculated by the PSO. The dependency of the δ_{hyper} and δ_{hypo} parameters are showcased by plotting combinations around the optimized values. The optimization resulted in a much stricter policy regarding hypoglycemia compared to hyperglycemia. This is an expected behavior, as the lower bound of the marked TIR zone is much closer to the nominal value.

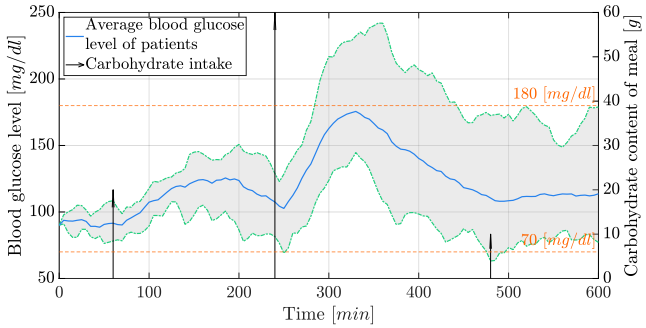

Fig. 7. Average blood glucose trajectory during a 10-hours long simulation.

In Fig. 7 simulated BG trajectories of the generated virtual patient cohort are shown (left axis). The average trajectory is plotted with a blue line, while the minimum and maximum values are denoted by green lines. The arrows indicate the timestamp and amount of the meals (right axis). Despite the fact that an announced meal scenario is investigated, due to the higher patient parameter variability and the CGMS noise postprandial hyperglycemic and short hypoglycemic events occurred.

A CGVA plot is provided in Fig. 8, representing the minimum and maximum values in the simulated horizon. With the exception of two patients, the investigated cohort lies in the B regions.

The (mean±standard deviation) percentage time spent in glucose range 70-180 $[mg/dL]$ of 10 virtual patients were 95.2±7.9 and 96.1±9.0 with and without CGM noise, respectively. The percentage time below range were 0.4±0.9 and 0.0±0.0. In this study, we applied only 10 virtual patients, since the purpose of the study was the development of the controller setup in an environment

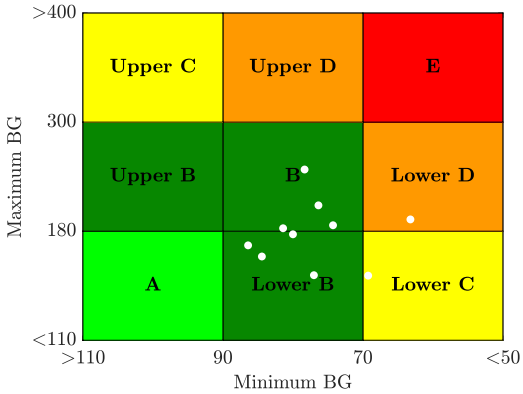

Fig. 8. Control variability grid analysis.

where the controller parameters are investigated, and tuned with an optimization method. During our further work, larger population and intrapatient variability is planned to be taken into account.

4. DISCUSSION AND CONCLUSION

In this study our aim was to develop a RHC application without the usual design and stability drawbacks of such a controller, which is able to handle higher parameter uncertainties and robust enough while keeping the control architecture and the applied models as simple, but as realistic as possible. In this first study, we investigated the case when both the insulin and meal intakes were "announced", namely, considered during the prediction done by the controller. The RHC parameter tuning was done by using a PSO algorithm. We developed simple fitting function Ψ to maximize the TIR. The controller design and control parameter optimization were done by using the average patient by considering the mean of the identified patients from Kanderian et al. (2009) and the tuned controller was tested on a virtual cohort generated by using 25% parameter variability in all parameters of (9)-(13) and the virtual cohort was extended by CGMS model as well with higher noise ($\omega \sim \mathcal{N}(0, 3.2^2)$). The PSO optimization run smoothly and found acceptable control parameters with respect the fitting function Ψ. It has to be noted that due to the multiple optimizations (in the PSO and in the RHC) we experienced increasing computational cost by extending the prediction horizon and simulated horizon.

We evaluated the results by using CVGA (Fig. 8) and TIR metrics where the total simulated horizons were represented with respect to the patient cohort (10 virtual patients are represented by the 10 white dots in Fig. 8). For the majority of patients a good TIR value is achieved, however there are some outliers in the cohort, where hyper- and/or hypoglycemic events occurs. Since variability applied in all the patient parameters, their effect on the BG trajectory and consequently on the TIR metric can mitigate or conversely, amplify their joint effect. This joint amplification can cause outliers, as it can be seen in the Lower C and D sections in the CVGA plot as well. According to our analysis, the outliers are caused by the joint effects of the randomized patient parameters related to the effect of insulin sensitivity and insulin clearance.

According to the evaluation, the developed RHC-based controller is able to provide satisfactory control performance.

In our further work we will develop a more complex cost function structure, furthermore, include a parameter estimation solution for online parameter estimation.

ACKNOWLEDGEMENTS

Supported by the Applied Informatics and Applied Mathematics Doctoral School of Óbuda University and the Robotics Special College of Óbuda University.

REFERENCES

Breton, M.D. and Kovatchev, B.P. (2021). One Year Real-World Use of Control-IQ Advanced Hybrid Closed-Loop Technology. *Diabetes Technology & Therapeutics*. doi: 10.1089/dia.2021.0097. Publisher: Mary Ann Liebert, Inc., publishers.

Brun, R., Reichert, P., and Künsch, H.R. (2001). Practical identifiability analysis of large environmental simulation models. *Water Resources Research*, 37(4), 1015–1030. doi:https://doi.org/10.1029/2000WR900350.

Castle, J. (2021). A Randomized, Two-way, Cross-over Study to Assess the Efficacy of an MPC Exercise-enabled Closed-loop System vs FMPD Exercise-enabled Closed-loop System. Clinical trial registration NCT04771403, clinicaltrials.gov. Submitted: January 27, 2021.

Colmegna, P.H., Bianchi, F.D., and Sánchez-Peña, R.S. (2021). Automatic Glucose Control During Meals and Exercise in Type 1 Diabetes: Proof-of-Concept in Silico Tests Using a Switched LPV Approach. *IEEE Control Systems Letters*, 5(5), 1489–1494. doi:10.1109/LCSYS.2020.3041211. Conference Name: IEEE Control Systems Letters.

Doyle, F.J., Huyett, L.M., Lee, J.B., Zisser, H.C., and Dassau, E. (2014). Closed-loop artificial pancreas systems: Engineering the algorithms. *Diab Care*, 37(5), 1191 – 1197.

Forlenza, G.P., Buckingham, B.A., Christiansen, M.P., Wadwa, R.P., Peyser, T.A., Lee, J.B., O'Connor, J., Dassau, E., Huyett, L.M., Layne, J.E., and Ly, T.T. (2019). Performance of Omnipod Personalized Model Predictive Control Algorithm with Moderate Intensity Exercise in Adults with Type 1 Diabetes. *Diabetes Technology & Therapeutics*, 21(5), 265–272. doi:10.1089/dia.2019.0017.

González, A.H., Rivadeneira, P.S., Ferramosca, A., Magdelaine, N., and Moog, C.H. (2020). Stable impulsive zone model predictive control for type 1 diabetic patients based on a long-term model. *Optimal Control Applications and Methods*, 41(6), 2115–2136. doi:https://doi.org/10.1002/oca.2647.

Hedrea, E.L., Precup, R.E., Roman, R.C., and Petriu, E.M. (2021). Tensor product-based model transformation approach to tower crane systems modeling. *Asian Journal of Control*. doi:https://doi.org/10.1002/asjc.2494.

Hovorka, R., Canonico, V., Chassin, L.J., Haueter, U., Massi-Benedetti, M., Federici, M.O., Pieber, T.R., Schaller, H.C., Schaupp, L., Vering, T., and Wilinska, M.E. (2004). Nonlinear model predictive control of glucose concentration in subjects with type 1 diabetes. *Physiol. Meas.*, 25(4), 905–920. doi:10.1088/0967-3334/25/4/010.

Huyett, L.M., Dassau, E., Zisser, H.C., and Doyle, F.J. (2018). Glucose sensor dynamics and the artificial pancreas: The impact of lag on sensor measurement and controller performance. *IEEE Control Systems Magazine*, 38(1), 30–46. doi:10.1109/MCS.2017.2766322.

Incremona, G.P., Messori, M., Toffanin, C., Cobelli, C., and Magni, L. (2018). Model predictive control with integral action for artificial pancreas. *Control Engineering Practice*, 77, 86–94. doi:10.1016/j.conengprac.2018.05.006.

Kanderian, S.S., Weinzimer, S., Voskanyan, G., and Steil, G.M. (2009). Identification of Intraday Metabolic Profiles during Closed-Loop Glucose Control in Individuals with Type 1 Diabetes. *J Diabetes Sci Technol*, 3(5), 1047–1057. doi:10.1177/193229680900300508.

Kennedy, J. and Eberhart, R. (1995). Particle swarm optimization. In *Proceedings of ICNN'95 - International Conference on Neural Networks*, volume 4, 1942–1948 vol.4. IEEE. doi:10.1109/ICNN.1995.488968.

Kovacs, L., Eigner, G., Siket, M., and Barkai, L. (2019). Control of Diabetes Mellitus by Advanced Robust Control Solution. *IEEE Access*, 7, 125609–125622. doi:10.1109/ACCESS.2019.2938267.

Kwon, W.H. and Han, S.H. (2006). *Receding horizon control: model predictive control for state models*. Springer Science & Business Media.

Richalet, J., Rault, A., Testud, J., and Papon, J. (1978). Model predictive heuristic control: Applications to industrial processes. *Automatica*, 14(5), 413–428.

Shah, V., Shoskes, A., Tawfik, B., and Garg, S. (2014). Closed-loop system in the management of diabetes: Past, present, and future. *Diabetes Technol The*, 16(8), 477 – 490.

Shi, Y. and Eberhart, R. (1998). A modified particle swarm optimizer. In *1998 IEEE International Conference on Evolutionary Computation Proceedings. IEEE World Congress on Computational Intelligence (Cat. No.98TH8360)*, 69–73. IEEE. doi:10.1109/ICEC.1998.699146.

Tamayo, M.F.V., Alvarez, M.A.C., and Rivadeneira, P. (2019). Handling parameter variations during the treatment of type 1 diabetes mellitus: In silico results. *Mathematical Problems in Engineering*, 2019, 1–21.

Vettoretti, M., Battocchio, C., Sparacino, G., and Facchinetti, A. (2019). Development of an error model for a factory-calibrated continuous glucose monitoring sensor with 10-day lifetime. *Sensors*, 19(23). doi:10.3390/s19235320.

Wright, E.E., Morgan, K., Fu, D.K., Wilkins, N., and Guffey, W.J. (2020). Time in Range: How to Measure It, How to Report It, and Its Practical Application in Clinical Decision-Making. *Clinical Diabetes*, 38(5), 439–448. doi:10.2337/cd20-0042. Publisher: American Diabetes Association.